


Article

Vorontsovite, $(\text{Hg}_5\text{Cu})_{\Sigma 6}\text{TlAs}_4\text{S}_{12}$, and Ferrovorontsovite, $(\text{Fe}_5\text{Cu})_{\Sigma 6}\text{TlAs}_4\text{S}_{12}$: The Tl- and Tl-Fe-Analogues of Galkhaite from the Vorontsovskoe Gold Deposit, Northern Urals, Russia

Anatoly V. Kasatkin ^{1,*}, Fabrizio Nestola ², Atali A. Agakhanov ¹, Radek Škoda ³ , Vladimir Y. Karpenko ¹, Mikhail V. Tsyganko ⁴ and Jakub Plášil ⁵

¹ Fersman Mineralogical Museum of Russian Academy of Sciences, Leninsky Prospekt 18-2, 119071 Moscow, Russia; atali99@mail.ru (A.A.A.); mineralab@mail.ru (V.Y.K.)

² Dipartimento di Geoscienze, Università di Padova, Via Gradenigo 6, I-35131 Padova, Italy; fabrizio.nestola@unipd.it

³ Department of Geological Sciences, Faculty of Science, Masaryk University, Kotlářská 2, 611 37 Brno, Czech Republic; rskoda@sci.muni.cz

⁴ ul. 40 Let Oktyabra 15, Kalya, 624474 Severouralsk, Sverdlovskaya Oblast', Russia; zigankom@mail.ru

⁵ Institute of Physics ASCR, v. v. i., Na Slovance 1999/2, 18221 Praha 8, Czech Republic; plasil@fzu.cz

* Correspondence: anatoly.kasatkin@gmail.com; Tel.: +7-916-179-10-32

Received: 11 April 2018; Accepted: 25 April 2018; Published: 28 April 2018



Abstract: Two new mineral species, vorontsovite, ideally $(\text{Hg}_5\text{Cu})\text{TlAs}_4\text{S}_{12}$, and ferrovorontsovite, ideally $(\text{Fe}_5\text{Cu})\text{TlAs}_4\text{S}_{12}$, the Tl- and Tl-Fe-analogues of galkhaite, respectively, have been discovered at the Vorontsovskoe gold deposit, Northern Urals, Russia. They occur as anhedral grains up to 0.5 mm (vorontsovite) and 0.2 mm (ferrovorontsovite) embedded in a calcite-dolomite matrix. The chemical composition of vorontsovite (wt %) is: Hg 35.70, Fe 5.36, Zn 1.26, Cu 3.42, Ag 0.64, Tl 11.53, Cs 0.35, Pb 0.04, As 15.98, Sb 2.35, Te 0.41, S 22.70, Se 0.02, total 99.76. The empirical formula, calculated on the basis of 23 atoms *pfu*, is: $[(\text{Hg}_{3.02}\text{Fe}_{1.63}\text{Zn}_{0.33})_{\Sigma 4.98}(\text{Cu}_{0.91}\text{Ag}_{0.10})_{\Sigma 1.01}](\text{Tl}_{0.96}\text{Cs}_{0.04})_{\Sigma 1.00}(\text{As}_{3.62}\text{Sb}_{0.33}\text{Te}_{0.05})_{\Sigma 4.00}\text{S}_{12.01}$. The composition of ferrovorontsovite (wt %) is: Hg 25.13, Fe 9.89, Zn 1.16, Cu 3.95, Ag 0.45, Tl 12.93, Cs 0.44, Pb 0.04, As 17.83, Sb 2.15, Te 0.40, S 24.91, total 99.28. The empirical formula, calculated on the basis of 23 atoms *pfu*, is: $[(\text{Fe}_{2.74}\text{Hg}_{1.94}\text{Zn}_{0.27})_{\Sigma 4.95}(\text{Cu}_{0.96}\text{Ag}_{0.06})_{\Sigma 1.02}](\text{Tl}_{0.98}\text{Cs}_{0.05})_{\Sigma 1.03}(\text{As}_{3.68}\text{Sb}_{0.27}\text{Te}_{0.05})_{\Sigma 4.00}\text{S}_{12.00}$. Both minerals are cubic, space group *I-43m*, with $a = 10.2956(6)$ Å, $V = 1091.3(1)$ Å³, $Z = 2$ (vorontsovite); and $a = 10.2390(7)$ Å, $V = 1073.43(22)$ Å³, $Z = 2$ (ferrovorontsovite). The crystal structures of both minerals were refined to $R = 0.0376$ (vorontsovite) and $R = 0.0576$ (ferrovorontsovite). Vorontsovite and ferrovorontsovite have been approved by the IMA-CNMNC under the numbers 2016-076 and 2017-007, respectively. The first one is named after the type locality, but also honors the mining engineer Vladimir Vasilyevich Vorontsov. The second is named for its chemical composition, as the Fe-analogue of the first. Both species are isostructural with galkhaite, being its Tl- and Tl-Fe analogues, respectively, and forming altogether the galkhaite group.

Keywords: vorontsovite; ferrovorontsovite; new minerals; thallium; chemistry; crystal structure; galkhaite group; Vorontsovskoe gold deposit

1. Introduction

Over the last few years, we have been systematically investigating a remarkable Tl-Hg-rich assemblage found in the specimens from the active Vorontsovskoe gold deposit in the Northern Urals. Our studies resulted in the discovery of several very rare minerals, such as bernardite [1],

chabournéite [2], christite [3], dalnegroite [4], parapierrotite [5], picotpaulite [6], sicherite [7], etc., but also yielded three new Tl-bearing minerals already approved by IMA-CNMNC (vorontsovite and ferrovorontsovite, described herein, and tsygankoite, described in another paper of the same special issue) while a few other potentially new species are still under investigation.

In this paper we describe two new minerals—vorontsovite (pronounced: vo-ron-tso-vait) and its Fe-analogue ferrovorontsovite (pronounced: fer-ro-vo-ron-tso-vait). Both were discovered in the specimens collected in March 2016 by one of the authors (M.V.T.) in the ore stockpile of the Vorontsovskoe deposit. Vorontsovite is named after its type locality, the Vorontsovskoe gold deposit, but also honors the mining engineer Vladimir Vasilyevich Vorontsov (1842–after 1908). V.V. Vorontsov was an important figure in the Northern Urals at the end of the 19th century; in particular, he was the superintendent of the Bogoslovskiy mining district where he organized an extensive geological survey and prospecting work that resulted in the discovery of several deposits, including an iron deposit. The mining settlement founded nearby in order to exploit that deposit and the iron deposit itself were named after V.V. Vorontsov—Vorontsovka and Vorontsovskoe, respectively. A gold deposit, discovered in 1985, neighbors the iron deposit, and was named after the nearest settlement, Vorontsovka. Consequently, we might conclude that, even if indirectly, the Vorontsovskoe gold deposit also honors V.V. Vorontsov. Ferrovorontsovite is named for its chemical composition, as the Fe analogue of vorontsovite.

Both minerals and their names have been approved by the Commission on New Minerals, Nomenclature and Classification (CNMNC) of the IMA, under the numbers 2016-076 and 2017-007, respectively. The type specimens of both new minerals are deposited in the collections of the Fersman Mineralogical Museum of the Russian Academy of Sciences, Moscow, Russia: vorontsovite—under the registration number 4917/1, and ferrovorontsovite—under the registration number 4976/1.

2. Occurrence

The Vorontsovskoe gold deposit is located 0.5 km west of the settlement of Vorontsovka, approximately 13 km south of the city of Krasnotur'insk, Sverdlovskaya Oblast, Northern Urals, Russia (59°39'5" N, 60°12'56" E). Vorontsovskoe gold deposit was discovered in 1985 and is currently operated by the Russian mining company "Polymetal International PLC" for high-grade gold-bearing ore. The ore reserves on 1 January 2016 were estimated at 0.9 mln. tr.oz of gold and an average content of 2.7 g/t. Geologically, the Vorontsovskoe deposit is located on the eastern slope of the Northern Urals in a sublongitudinal volcanic-plutonic belt bound by faults [8]. Ore formation developed in several stages and resulted in the existence of several mineral types of ore. Three main types of primary ores can be selected according to their mineral composition, geochemical specialization, and time of formation: (1) sulfide-skarn ores; (2) sulfide-silicate ores; and (3) sulfide-carbonate ores. In all cases the productive sulfide mineralization associates with particular metasomatic rocks [9].

Vorontsovite and ferrovorontsovite were found in the ores of the third, sulfide-carbonate type. They comprise limestone breccias (calcite-dolomite, up to 84.5% of volume), main silicate minerals (quartz, feldspar, clinocllore, muscovite, up to 10% of volume), accessory minerals (titanite, apatite, baryte, armenite, scheelite, gold), and sulfidic assemblage. The latter demonstrates a large variety of mineral species. Pyrite, realgar, stibnite, and cinnabar are abundant; orpiment, sphalerite (including Hg-bearing variety), and metacinnabar (Zn–Mn-bearing) are less common, while wakabayashilite (As,Sb)₆As₄S₁₄ and coloradoite HgTe are rare. Thallium mineralization is presented by relatively common routhierite TlCuHg₂As₂S₆, dalnegroite (Tl₄Pb₂(As,Sb)₂₀S₃₄)—chabournéite (Tl₄Pb₂(Sb,As)₂₀S₃₄) and parapierrotite (TlSb₅S₈)—bernardite (TlAs₅S₈) series. It is interesting to note that in these two pairs showing As–Sb isomorphism, dalnegroite (As > Sb) is found much more often than chabournéite, while in the second pair, instead, parapierrotite (Sb > As) shows to be very common locally while bernardite is much rarer. Other Tl-bearing species are extremely rare and include christite TlHgAsS₃, boscardinite TlPb₄(Sb₇As₂)_{Σ=9}S₁₈ and minerals of the sartorite group (enneasartorite Tl₆Pb₃₂As₇₀S₁₄₀ and heptasartorite Tl₇Pb₂₂As₅₅S₁₀₈). Vorontsovite and ferrovorontsovite themselves

should be considered as rare, though in a couple of samples their segregations were found to be relatively abundant.

The Vorontsovskoe gold deposit is a type locality for another rare mineral, clerite MnSb_2S_4 [10], but it was not observed in the same association with vorontsovite and ferrovorontsovite.

3. Physical and Optical Properties

Vorontsovite and ferrovorontsovite occur as black anhedral grains and their segregations embedded in white calcite-dolomite matrix (Figure 1). Individual grains are up to 0.5 mm and 0.2 mm across, respectively, but usually much smaller (average size of both—0.05 mm across); segregations are up to 1 mm (Figure 2a,b).

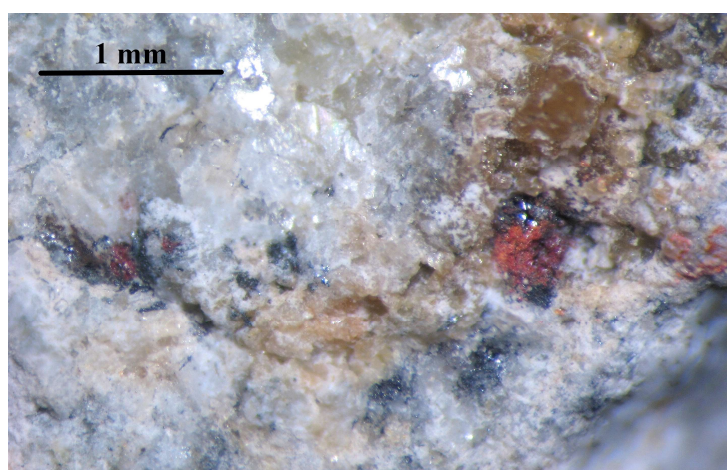


Figure 1. Grains of vorontsovite (black with metallic luster) with red cinnabar in white dolomite-calcite matrix. The brownish-orange material is also calcite.

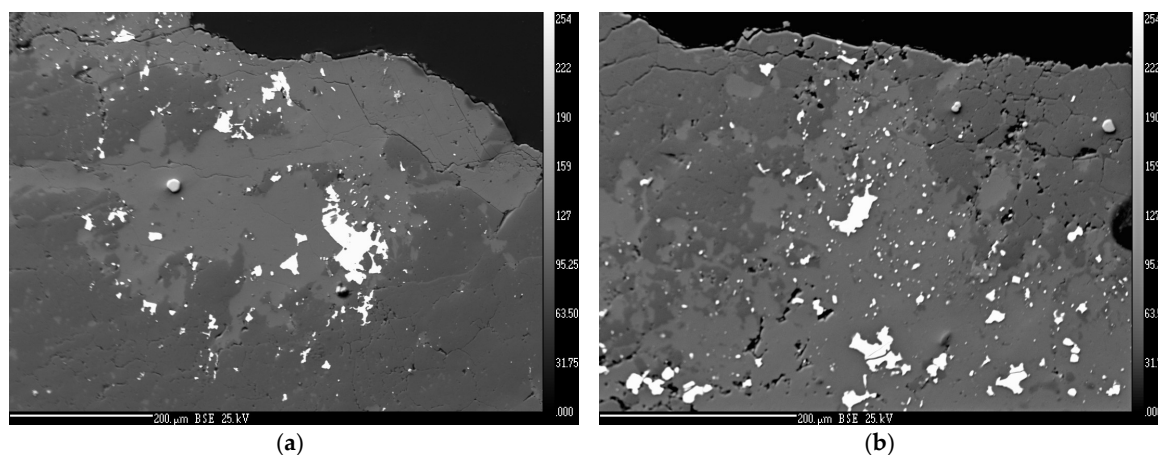


Figure 2. SEM (BSE) images showing: (a) vorontsovite; and (b) ferrovorontsovite grains (both-white) in calcite (medium-grey) and dolomite (dark-grey) matrix. Small whitish-grey rounded crystals are pyrite. Polished sections.

Both species are opaque in transmitted light and exhibit metallic luster and black streak. Their tenacity is brittle and their fracture is uneven. Cleavage and parting were not observed. Both are non-fluorescent. Their Vickers hardness (VHN_{10}) is 172 kg/mm^2 (range 166–178) for vorontsovite and 170 kg/mm^2 (range 166–174) for ferrovorontsovite, corresponding to a Mohs hardness of $\sim 3\frac{1}{2}$. Their density could not be measured because of the absence of suitable heavy liquids. Their calculated

density (for $Z = 2$) based on the empirical formulae and unit-cell volume from single-crystal X-ray diffraction data is $5.140 \text{ g}\cdot\text{cm}^{-3}$ for vorontsovite and $4.744 \text{ g}\cdot\text{cm}^{-3}$ for ferrovorontsovite.

In reflected light both species are light grey; between crossed polars they are black and isotropic. No birefractance, pleochroism, and internal reflections are observed. Quantitative reflectance measurements were performed in air relative to a WTiC standard by means of a Universal Microspectrophotometer UMSP 50 (Opton-Zeiss, Germany) (Table 1).

Table 1. Reflectance data for vorontsovite (1) and ferrovorontsovite (2).

λ (nm)	R (%)	
	1	2
400	25.62	24.90
420	25.82	25.02
440	25.97	25.21
460	26.20	25.43
470	26.31	25.54
480	26.42	25.64
500	26.54	25.87
520	26.95	26.11
540	27.21	26.41
546	27.30	26.49
560	27.55	26.71
580	27.87	27.06
589	28.11	27.26
600	28.30	27.47
620	28.70	27.52
640	29.06	27.83
650	29.28	27.90
660	29.47	27.98
680	29.98	28.39
700	30.44	28.83

Note: Reflectance percentages for the four COM (Commission on Ore Mineralogy) wavelengths are given in bold.

4. Chemical Composition and Chemical Properties

Preliminary chemical analyses using a CamScan 4D scanning electron microscope (Oxford Instruments, Abingdon, UK) equipped with an INCA Energy microanalyzer (EDS mode, 20 kV, 5 nA and beam diameter 5 μm) showed the presence in vorontsovite of Tl, Hg, Fe, Zn, Cu, As, Sb, minor Cs, Ag, Te, and traces of Pb and Se. The same elements, except Se, were detected in ferrovorontsovite. No other elements with atomic numbers higher than 8 were detected.

Quantitative chemical analyses were conducted in wavelength-dispersive (WDS) mode, using a Cameca SX-100 electron microprobe (Cameca company, Paris, France) operating at 25 kV and 20 nA with a beam size of 1 μm . Peak counting times were 20 s for all elements, with one half of the peak time for each background. The following standards, X-ray lines and analyzing crystals (in parentheses) were used: Hg—HgTe, $M\alpha$ (LPET); Fe—FeS₂, $K\alpha$ (LLIF); Zn—ZnS, $K\alpha$ (LLIF); Cu—Cu metal, $K\alpha$ (LLIF); Ag—Ag metal, $L\alpha$ (PET); Tl—Tl(Br,I), $M\alpha$ (PET); Cs—pollucite, $L\alpha$ (LPET); Pb—PbSe, $M\alpha$ (LPET); As—pararammelsbergite, $L\beta$ (TAP); Sb—Sb, $L\beta$ (PET); Te—HgTe, $L\beta$ (LPET); S—chalcopyrite, $K\alpha$ (LPET); Se—PbSe, $L\beta$ (TAP). Analytical data are given in Table 2 (the mean of 10 spot analyses for each species; range, and the standard deviation).

The empirical formula of vorontsovite (based on 23 atoms *pfu*) is: $[(\text{Hg}^{2+}_{3.02}\text{Fe}^{2+}_{1.63}\text{Zn}_{0.33})_{\Sigma 4.98}(\text{Cu}^{+}_{0.91}\text{Ag}_{0.10})_{\Sigma 1.01}](\text{Tl}^{+}_{0.96}\text{Cs}_{0.04})_{\Sigma 1.00}(\text{As}_{3.62}\text{Sb}_{0.33}\text{Te}_{0.05})_{\Sigma 4.00}\text{S}_{12.01}$. Its ideal chemical formula is $(\text{Hg}_5\text{Cu})_{\Sigma 6}\text{TlAs}_4\text{S}_{12}$, which requires Hg 51.33, Cu 3.24, Tl 10.42, As 15.34, S 19.67, total 100.00 wt %. The empirical formula of ferrovorontsovite (based on 23 atoms *pfu*) is: $[(\text{Fe}^{2+}_{2.74}\text{Hg}^{2+}_{1.94}\text{Zn}_{0.27})_{\Sigma 4.95}(\text{Cu}^{+}_{0.96}\text{Ag}_{0.06})_{\Sigma 1.02}](\text{Tl}^{+}_{0.98}\text{Cs}_{0.05})_{\Sigma 1.03}(\text{As}_{3.68}\text{Sb}_{0.27}\text{Te}_{0.05})_{\Sigma 4.00}\text{S}_{12.00}$. Its ideal chemical formula is $(\text{Fe}_5\text{Cu})\text{TlAs}_4\text{S}_{12}$, which requires Fe 22.67, Cu 5.18, Tl 16.57, As 24.32, S 31.26, total 100.00 wt %.

Several vorontsovite and ferrovorontsovite grains were carefully extracted from the calcite-dolomite matrix by the aid of dilute 10% HCl and showed to be totally insoluble in acids and alkalis.

Table 2. Chemical data for vorontsovite and ferrovorontsovite.

Constituent	Vorontsovite			Ferrovorontsovite		
	wt %	Range	SD	wt %	Range	SD
Hg	35.70	30.66–38.78	3.18	25.13	22.03–27.00	1.53
Fe	5.36	3.99–8.46	1.63	9.89	9.08–10.88	0.53
Zn	1.26	1.16–1.35	0.05	1.16	0.93–1.43	0.19
Cu	3.42	3.28–3.75	0.16	3.95	3.84–4.07	0.08
Ag	0.64	0.47–0.85	0.12	0.45	0.10–0.89	0.22
Tl	11.53	10.93–12.27	0.45	12.93	12.22–13.55	0.55
Cs	0.35	0–0.67	0.25	0.44	0.19–0.78	0.22
Pb	0.04	0–0.11	0.04	0.04	0–0.09	0.04
As	15.98	14.74–17.26	0.95	17.83	17.13–19.01	0.60
Sb	2.35	1.58–2.79	0.52	2.15	1.59–2.85	0.35
Te	0.41	0.36–0.49	0.04	0.40	0.38–0.50	0.04
S	22.70	21.91–24.31	0.75	24.91	23.90–25.90	0.57
Se	0.02	0–0.08	0.03	b.d.l.		
Total	99.76			99.28		

Note: SD = standard deviation; b.d.l. = below detection limits.

5. X-ray Crystallography

Single-crystal X-ray studies of vorontsovite and ferrovorontsovite were carried out on grains of 0.015 mm × 0.012 mm × 0.010 mm and 0.020 mm × 0.010 mm × 0.008 mm, respectively, using a Rigaku-Oxford-Diffraction Supernova diffractometer equipped with a Dectris Pilatus 200K detector. The instrument is equipped with a Mo micro-focus X-ray tube, working at 50 kV and 0.8 mA (40 W), providing a beam spot of 120 μm [11]. For vorontsovite we have collected 1257 frames by 25 runs using an omega scan mode and an exposure time of 10 s. The data were collected up to $2\theta_{\max} = 60^\circ$. The unit-cell edge was determined using 1342 observed reflections. The following data were obtained: vorontsovite is cubic, $a = 10.2956(6)$ Å, $V = 1091.3(1)$ Å³, $Z = 2$ with space group: $I-43m$. For ferrovorontsovite we have collected 657 frames by 12 runs using an omega scan mode for about 22 h. Data was collected up to $2\theta_{\max} = 60^\circ$. The unit-cell edge resulted to be the following: cubic, $a = 10.2390(7)$ Å, $V = 1073.43(22)$ Å³, $Z = 2$ with space group: $I-43m$.

The X-ray instrument mentioned above was used as a micro-powder diffractometer and allowed us to collect the powder diffraction data for both minerals. A standard phi scan mode, as implemented in the powder power tool of CrysAlis Pro, was used for the powder data collection. A complete list of observed d spacings and relative intensities compared with the calculated ones (obtained from the single-crystal structure refinement) is reported in Table 3. The unit-cell edge and volume of vorontsovite obtained by using the d spacing values reported in Table 3, and the software UnitCell by Holland and Redfern [12] are: cubic, $a = 10.2921(2)$ Å, $V = 1090.21(5)$ Å³, $Z = 2$, space group: $I-43m$. The difference in volume from the powder data collection with respect to the single-crystal data is of only about 0.1%.

The unit-cell edge and volume of ferrovorontsovite obtained by using the d spacing values reported in Table 3 and the above mentioned software are: cubic, $a = 10.2486(2)$ Å, $V = 1076.46(6)$ Å³, $Z = 2$, space group: $I-43m$. The difference in volume from the powder data collection with respect to the single-crystal data is of only about 0.3%.

Table 3. Powder X-ray data for vorontsovite and ferrovorontsovite. The five strongest diffraction lines are given in bold.

Vorontsovite				Ferrovorontsovite				<i>h k l</i>
<i>I</i> _{obs}	<i>d</i> _{obs} (Å)	<i>I</i> _{calc}	<i>d</i> _{calc}	<i>I</i> _{obs}	<i>d</i> _{obs} (Å)	<i>I</i> _{calc}	<i>d</i> _{calc}	
16	7.280	14	7.280	10	7.220	10	7.240	1 1 0
79	4.198	85	4.203	93	4.175	81	4.180	2 1 1
14	3.676	9	3.640	13	3.646	14	3.620	2 2 0
100	2.970	100	2.972	100	2.952	100	2.956	2 2 2
66	2.749	70	2.752	57	2.735	66	2.736	3 2 1
22	2.572	31	2.574	18	2.562	24	2.560	4 0 0
6	2.425	5	2.427	8	2.417	6	2.414	4 1 1, 3 3 0
8	2.191	9	2.195	7	2.182	2.183	7	3 3 2
20	2.017	14	2.019	8	2.069	2.090	3	4 3 1, 5 1 0
18	1.879	15	1.880	11	1.869	1.869	14	5 2 1
49	1.818	54	1.820	40	1.810	1.810	55	4 4 0
9	1.762	4	1.766	9	1.760	1.756	4	4 3 3, 5 3 0
14	1.670	8	1.670	8	1.661	1.661	8	5 3 2, 6 1 1
8	1.591	3	1.589	2	1.580	1.580	2	5 4 1
31	1.550	34	1.552	24	1.543	1.544	33	6 2 2
7	1.486	6	1.486	2	1.479	1.478	5	4 4 4
8	1.453	3	1.456	4	1.450	1.448	2	5 4 3, 7 1 0
8	1.397	2	1.401	3	1.394	1.393	2	6 3 3, 5 5 2, 7 2 1
10	1.298	2	1.308	1	1.304	1.300	2	8 0 0
5	1.230	3	1.231	2	1.226	1.224	3	6 5 3
4	1.200	1	1.197	4	1.190	1.190	2	6 6 2
8	1.180	10	1.181	7	1.176	1.174	9	7 5 2
8	1.150	6	1.151	2	1.150	1.145	4	8 4 0
2	1.050	6	1.051	3	1.046	1.045	6	8 4 4
2	0.989	3	0.991	2	0.987	0.985	3	6 6 6, 10 2 2

List of *d* spacings (observed, *d*_{obs}, and calculated, *d*_{calc}) and relative intensity (%) from powder diffraction data for vorontsovite and ferrovorontsovite. Calculated intensity and *d*_{calc} were obtained from Powdercell software [13] using the crystal structure model of Tables 5 and 6.

6. Description of the Crystal Structures

The crystal structures of vorontsovite and ferrovorontsovite were refined to $R = 0.0376$ for 227 observed reflections and to $R = 0.0576$ for 250 observed reflections, respectively. The data were processed using CrysAlis Pro (Rigaku-Oxford Diffraction) applying the Lorentz-Polarization correction and the interframe scaling for the empirical absorption correction. The crystal structure refinements were performed by using SHELXL [14] starting from the model of Biagioni et al. [15], who investigated three different samples of galkhaite from the USA, Russia, and Italy, and the less recent, but very reliable, paper of Chen and Szymański [16], who studied 47 crystals of galkhaite from the USA. We must mention an even older work on galkhaite [17]. Crystal and refinement data for vorontsovite and ferrovorontsovite are reported in Table 4; atomic coordinates and selected bond distances are reported in Tables 5 and 6.

The analysis of the systematic absences of vorontsovite and ferrovorontsovite definitively confirmed the same space group proposed by Chen and Szymański [16] and Biagioni et al. [15] for galkhaite being $I-43m$.

Similarly to galkhaite, the crystal structure of vorontsovite (Figure 3) is represented by three independent crystallographic sites.

Table 4. Crystal data and refinement details for vorontsovite and ferrovorontsovite.

Crystal Data	Vorontsovite	Ferrovorontsovite
Crystal size (mm ³)	0.015 × 0.012 × 0.010	0.020 × 0.010 × 0.008
Cell setting, space group	Cubic, <i>I-43m</i>	Cubic, <i>I-43m</i>
<i>a</i> (Å)	10.2956(6)	10.2390(7)
<i>V</i> (Å ³)	1091.32(11)	1073.43(22)
<i>Z</i>	2	2
Data collection and refinement		
Radiation, wavelength (Å)	Mo <i>K</i> α, λ = 0.71073	Mo <i>K</i> α, λ = 0.71073
Temperature (K)	298	298
2θ _{max} (°)	60.02	59.75
Measured reflections	12180	6329
Unique reflections	315	312
Reflections with <i>F</i> _o > 4σ(<i>F</i> _o)	227	250
Range of <i>h, k, l</i>	−14 ≤ <i>h</i> ≤ 14, −14 ≤ <i>k</i> ≤ 14, −14 ≤ <i>l</i> ≤ 14	−14 ≤ <i>h</i> ≤ 14, −14 ≤ <i>k</i> ≤ 14, −14 ≤ <i>l</i> ≤ 14
<i>R</i> [<i>F</i> _o > 4σ(<i>F</i> _o)]	0.0376	0.0576
<i>R</i> (all data)	0.0624	0.0753
<i>wR</i> (on <i>F</i> ²)	0.0621	0.1235
Goof	1.044	1.144
Number of least-squares parameters	18	16

Table 5. Atomic coordinates, displacement parameters (Å²), and selected bond distances (Å) for vorontsovite.

Site	<i>x/a</i>	<i>y/b</i>	<i>z/c</i>	<i>U</i> _{eq}
Tl	0	0	0	0.336(7)
Hg	0	0.25	0.50	0.0428(4)
As	0.2420(2)	0.2420(2)	0.2420(2)	0.0292(8)
S	0.3870(2)	0.3870(2)	0.1573(4)	0.0355(13)
Tl	−S	3.893(4) × 12		
Hg	−S	2.443(2) × 4		
As	−S	2.283(4) × 3		

Table 6. Atomic coordinates, displacement parameters (Å²), and selected bond distances (Å) for ferrovorontsovite.

Site	<i>x/a</i>	<i>y/b</i>	<i>z/c</i>	<i>U</i> _{eq}
Tl	0	0	0	0.379(10)
Fe	0	0.25	0.50	0.0316(6)
As	0.2412(2)	0.2412(2)	0.2412(2)	0.0292(9)
S	0.3868(3)	0.3868(3)	0.1542(5)	0.0378(13)
Tl	−S	3.902(5) × 12		
Fe	−S	2.408(4) × 4		
As	−S	2.288(5) × 3		

(1) The Hg-site shows a tetrahedral coordination with the bond length being 2.443(2) Å against 2.473, 2.507, and 2.524 Å reported by the three samples of galkhaite analyzed by Biagioni et al. [15] and 2.496 Å for the sample of galkhaite studied by Chen and Szymansky [16]. The significant contraction of the vorontsovite Hg–S distance could be explained in terms of crystal chemistry: the Hg content in vorontsovite is significantly lower than that in galkhaite, and considering its cation radius (*r* = 0.96 Å in tetrahedral coordination [18]) with respect to other substituting cations like Cu, Fe, Zn, Ag [15,16] this is consistent with a general reduction of the Hg–S distance.

(2) The Tl-site is a 12-fold coordinated site. This site represents a large cavity and, as stated by [15], the coordination polyhedron could be described as a Laves polyhedron, a truncated tetrahedron.

The Tl–S distance in vorontsovite is 3.893(4) Å. This same site in galkhaite is Cs-dominant. In detail, for galkhaite reported by Biagioni et al. [15], the Cs–S distance varies between 3.874 and 3.884 Å. The Cs–S distance reported by Chen and Szymansky [18] is 3.863 Å. Thus, it is evident that, for the Tl/Cs site, the differences are very small, likely within two uncertainties.

(3) As is at the top of a trigonal pyramid, the base of which is a triangle formed by S-anions. Smaller triangular faces of the Tl Laves polyhedra are centered by As, which is lifted over the face, that is determined by the minimal possible Tl–As distances. The As–S distance in vorontsovite is 2.283(4) Å, which is a very similar value to those reported by Biagioni et al. [15] for their three samples (2.267, 2.286, and 2.270 Å) and by Chen and Szymansky [16] (2.265 Å).

In terms of matching between the site scattering values from the microprobe analysis (from the second column in Table 2) and that from the X-ray diffraction for vorontsovite we can remark that we found a very good agreement. The calculated electrons from the microprobe data are 54.3 for the Hg site, 80.0 for the Tl site, and 34.7 for the As site. From the X-ray data we obtained 51.7 for the Hg site, 83.4 for the Tl site and 34.6 for the As site. In total, the microprobe data provide 169 electrons relative to the cation contribution, whereas the X-ray data provide 169.7 electrons, a difference of about 0.4%.

Similarly to vorontsovite, the crystal structure of ferrovorontsovite (Figure 3) is represented by three independent crystallographic sites.

(1) The Fe-site shows a tetrahedral coordination with the bond length being 2.408(4) Å against 2.443 Å reported for vorontsovite. The significant contraction of ferrovorontsovite (Fe,Hg)–S distance with respect to vorontsovite can be explained in terms of crystal chemistry: the Hg content in ferrovorontsovite is significantly lower than that in vorontsovite and considering its cation radius ($r = 0.96$ Å in tetrahedral coordination [19]) with respect to Fe and other substituting cations like Cu, Zn, and Ag, this is consistent with a general reduction of such tetrahedral distance.

(2) The Tl-site is a 12-fold coordinated site. The Tl–S distance in ferrovorontsovite is 3.902(5) Å, which is practically identical (at least within 1–2 uncertainties) to that of vorontsovite, which is 3.893(4) Å.

(3) The As-site is a trigonal pyramid with As coordinating three S. The As–S distance in ferrovorontsovite is 2.284(5), again very similar to vorontsovite, which is 2.283(4) Å (one uncertainty different).

In terms of matching between the site scattering values from the microprobe analysis (from third column in Table 2) and that from the X-ray diffraction for ferrovorontsovite, we can remark that we found a very good agreement. The calculated electrons from the microprobe data are 44.2 for the Fe site, 82.1 for the Tl site, and 34.4 for the As site. From the X-ray data we obtained 43.8 for the Fe site, and full occupancy for the Tl site and the As site. In total, the microprobe data provide 160.7 electrons relative to the cation contribution, whereas the X-ray data provide 157.8 electrons. Taking into account the heavy elements in the structure and the crystal size of the sample investigated we consider such difference very satisfying.

For both vorontsovite and ferrovorontsovite, it is evident that the U_{eq} for the Tl site is definitively high. This could be explained (a) by a wrong assumption in terms of the electron density of the site (i.e., we assumed an electron density higher than the real one), but such a possibility is unlikely as the chemical data indicate a full occupancy of the Tl site (with $Tl \gg Cs$); or (b) by supporting the explanation provided by [15,16], who state in their works that the partial replacement of Cs^+ by the smaller Tl^+ cation would cause a large movement (indicated as rattling by [16]) of the (Cs,Tl) in the cavity. In vorontsovite and ferrovorontsovite, the Cs^+ / Tl^+ replacement is not partial, but nearly “total” and, therefore, the statement by [16], also supported by [15], could be the real cause of the strong displacement parameters for the Tl site in our samples. The possibility that the strong displacement parameter is due to a possible split position must be ruled out as any attempts to refine a split position for the Tl site provided a totally unreliable refinement.

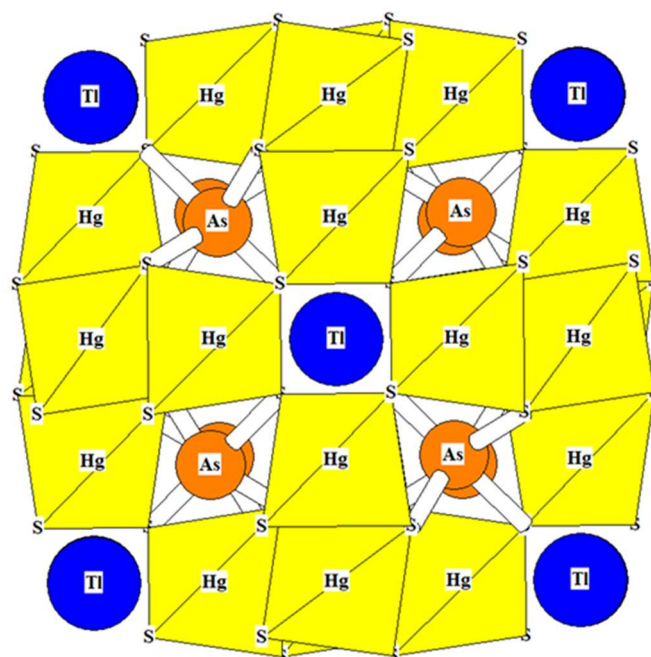


Figure 3. Crystal structure of vorontsovite/ferrovorontsovite viewed along the [001] direction. For simplicity, in the figure the site occupied by (Hg, Fe, Zn, Cu, Ag) is indicated as Hg, whereas the site occupied by Tl and Cs is indicated as Tl. Finally, the site occupied by As and Sb is indicated as As.

7. Discussion

Vorontsovite is the thallium analogue of galkhaite, ideally $(\text{Hg}_5\text{Cu})_{\Sigma 6}\text{CsAs}_4\text{S}_{12}$ [15,20]. Ferrovorontsovite is the iron analogue of vorontsovite and, consequently, the iron-thallium analogue of galkhaite. According to the group nomenclature [21] the galkhaite group should be established with galkhaite, vorontsovite, and ferrovorontsovite being its first three members. For comparison of all three minerals see Table 7.

Table 7. Comparative data for galkhaite from type locality, Gal-Khaya deposit, Sakha Republic, Russia, vorontsovite, and ferrovorontsovite.

Mineral	Galkhaite (from Gal-Khaya)	Vorontsovite	Ferrovorontsovite
End-member formula	$(\text{Hg}_5\text{Cu})\text{CsAs}_4\text{S}_{12}$	$(\text{Hg}_5\text{Cu})\text{TlAs}_4\text{S}_{12}$	$(\text{Fe}_5\text{Cu})\text{TlAs}_4\text{S}_{12}$
Empirical formula	$[(\text{Hg}_{4.66}\text{Zn}_{0.32})_{\Sigma 4.98}$ $(\text{Cu}_{0.55}\text{Ag}_{0.45})_{\Sigma 1.00}]$ $(\text{Cs}_{0.74}\text{Tl}_{0.06})_{\Sigma 0.80}$ $(\text{As}_{3.42}\text{Sb}_{0.56})_{\Sigma 3.98}\text{S}_{12.05}$	$[(\text{Hg}_{3.02}\text{Fe}_{1.63}\text{Zn}_{0.33})_{\Sigma 4.98}$ $(\text{Cu}_{0.91}\text{Ag}_{0.10})_{\Sigma 1.01}]$ $(\text{Tl}_{0.96}\text{Cs}_{0.04})_{\Sigma 1.00}$ $(\text{As}_{3.62}\text{Sb}_{0.33}\text{Te}_{0.05})_{\Sigma 4.00}\text{S}_{12.01}$	$[(\text{Fe}_{2.74}\text{Hg}_{1.94}\text{Zn}_{0.27})_{\Sigma 4.95}$ $(\text{Cu}_{0.96}\text{Ag}_{0.06})_{\Sigma 1.02}]$ $(\text{Tl}_{0.98}\text{Cs}_{0.05})_{\Sigma 1.03}$ $(\text{As}_{3.68}\text{Sb}_{0.27}\text{Te}_{0.05})_{\Sigma 4.00}\text{S}_{12.00}$
Crystal system	Cubic	Cubic	Cubic
Space group	$I-43m$	$I-43m$	$I-43m$
a , Å	10.443(1)	10.2956(6)	10.2390(7)
V , Å ³	1138.9(2)	1091.32(11)	1073.43(22)
Z	2	2	2
Strongest lines of the X-ray powder-diffraction pattern: d , Å- l , %	4.27–70 3.01–100 2.78–80 1.84–50	4.20–79 2.97–100 2.75–66 1.82–49	4.18–93 2.95–100 2.74–57 1.81–40

Table 7. Cont.

Mineral	Galkhaite (from Gal-Khaya)	Vorontsovite	Ferrovorontsovite
Color	Dark orange-red	Black	Black
Streak	Orange-yellow	Black	Black
Luster	Vitreous to adamantine	Metallic	Metallic
Hardness, kg/mm ² , mean (range)	190 (171–205)	172 (166–178)	170 (166–174)
Optical data	Light grey with bluish-lilac hue in reflected light Isotropic	Light grey in reflected light Isotropic	Light grey in reflected light Isotropic
Density, g·cm ⁻³	5.4 (meas.) 5.44 (calc.)	5.140 (calc.)	4.744 (calc.)
References	[15,19]	This study	This study

In the Nickel-Strunz classification system, vorontsovite and ferrovorontsovite fit in Subdivision 2.GB.20 in Dana classification 3.4.14.1.

The possible existence of a natural thallium-analogue of galkhaite was debated in the past by a few authors [15,22]. Chen and Szymański [18], in the course of their study of galkhaite from the Getchell Mine, NV, USA, reported the existence of one zoned crystal having Cs > Tl on its outermost zone, but Tl > Cs in the core. Microprobe analysis of that central part gave (in wt %): Hg 48.9, Cu 3.5, Zn 2.3, Tl 6.7, As 15.4, Sb 0.3, Cs 2.5, S 22.2, total 101.8. The recalculation on the basis of 23 atoms *pfu* yields the following empirical formula: [(Hg_{4.36}Zn_{0.63}) Σ 4.99Cu_{0.98}](Tl_{0.59}Cs_{0.34}) Σ 0.93(As_{3.68}Sb_{0.04}) Σ 3.72S_{12.38}, which corresponds formally to vorontsovite. Chen and Szymański [18] admitted, however, that peak overlapping and the lack of suitable standards might affect the accuracy of their chemical data. Indeed, if comparing with vorontsovite, the above formula has an obvious discrepancy in the As:S ratio while Hg, Cu, and (Tl + Cs) content are, in general, in conformity with our new mineral. It should be also noted that all following researchers who studied galkhaite from various localities did not find any other spots showing Tl dominance over Cs [15,22,23].

Chen and Szymański [18] reported a large inhomogeneity in the Cs:Tl ratio in galkhaite crystals from the Getchell mine showing a partial solid-solution series ranging from a Tl-free end-member to one spot of the formal vorontsovite, as noted above (see yellow squares in Figure 4). Other researchers of galkhaite, however, noted a rather limited substitution of Cs⁺ for Tl⁺. Similarly, at the Vorontsovskoe deposit the Tl–Cs isomorphism in the 12-fold coordinated site is very limited (Figure 4). The largest Cs content in vorontsovite detected by us was 0.67 wt %, corresponding to 0.09 *apfu* only. The same applies to ferrovorontsovite, where we registered a maximum 0.78 wt % of Cs, corresponding to 0.08 *apfu*.

Instead, we recorded, at the Vorontsovskoe deposit, a very large isomorphous substitution of Hg for Fe and partially by Zn in mixed tetrahedral sites leading to a continuous solid solution series from completely Fe–Zn-free vorontsovite, through many intermediates in the Hg/Fe ratio members, including those corresponding to the middle of the series, to the end-member Hg–Zn-free ferrovorontsovite (Figure 5).

The homovalent substitution Hg²⁺ ↔ Fe²⁺, Zn²⁺ is typical for many sulfosalts and has been observed, i.e., in fahlores; minerals of the stannite group, such as stannite (Fe-end member)—kësterite (Zn-end member)—velikite (Hg-end member); minerals of the routhierite group, such as routhierite (Hg-end member)—staldlerite (Zn-end member)—ferrostaldlerite (Fe-end member), etc. Vorontsovite (Hg-end member)—ferrovorontsovite (Fe-end member) pairs represent another example of such chemical substitution. While we did not record more than 1.43 wt % of Zn in ferrovorontsovite (0.33 *apfu*) and more than 1.35 wt % in vorontsovite (0.34 *apfu*), the possible existence in nature of “zincovorontsovite” (Zn-end member) cannot be excluded.

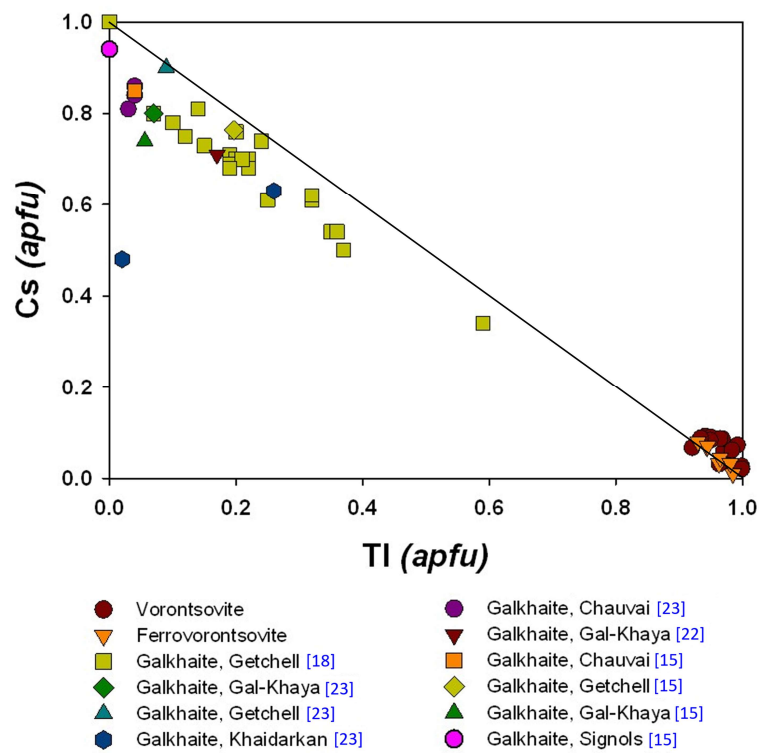


Figure 4. Tl vs. Cs, in *apfu*, in vorontsovite, ferrovorontsovite (our data), and galkhaite (various literature data obtained from samples from the Getchell mine, Nevada, USA; Gal-Khaya deposit, Sakha Republic, Russia; Khaidarkan deposit, Kyrgyzstan; Chauvai deposit, Kyrgyzstan; and Signols, Piedmont, Italy).

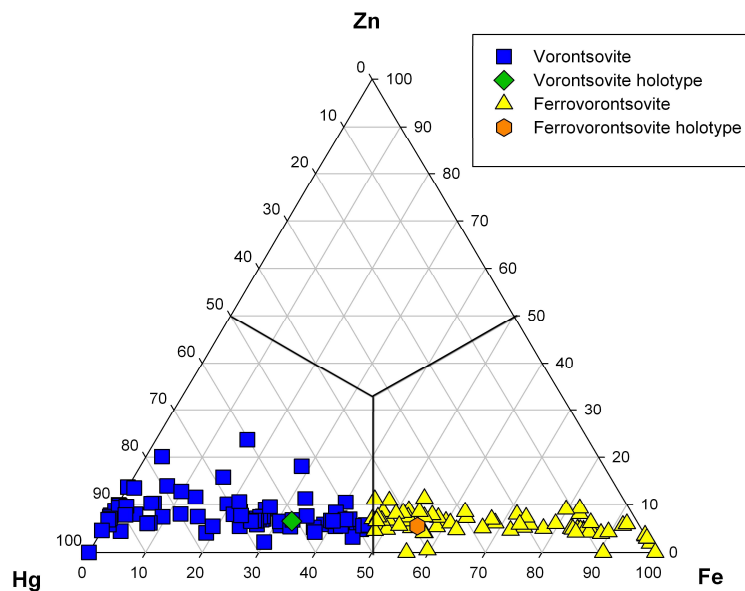


Figure 5. Ternary plot showing continuous solid solution series between vorontsovite (84 analyses) and ferrovorontsovite (73 analyses) at the Vorontsovskoe deposit.

8. General Conclusions

Although very rare, Tl-bearing minerals are attracting attention in mineralogy for several reasons, mainly related to the strong toxicity of Tl elements for living organisms and to the increased economic value that such elements have shown in the last 20 years (i.e., from 1278 \$/kg in 1995 to 7400 \$/kg in 2015 [24]). In this light, our work could cover an important role in the knowledge of Tl and Tl-bearing minerals, as vorontsovite and ferrovorontsovite are minerals characterized by significant amount of Tl with about 11 and 13 wt %, respectively.

In addition, in our knowledge, excluding vorontsovite and ferrovorontsovite, only six minerals exist with the simultaneous presence of Tl, Hg, and As in significant amounts (arsiccioite $\text{AgHg}_2\text{TlAs}_2\text{S}_6$ [25], christite TlHgAsS_3 [3], routhierite $\text{TlCuHg}_2\text{As}_2\text{S}_6$ [26], simonite $\text{TlHgAs}_3\text{S}_6$ [27], stalderite $\text{TlCu}(\text{Zn,Fe,Hg})_2\text{As}_2\text{S}_6$ [28], and vrbaite $\text{Hg}_3\text{Tl}_4\text{As}_8\text{Sb}_2\text{S}_{20}$ [29]). Mercury, thallium, and arsenic also represent crucial elements in environmental hazards and, thus, it is evident that works like ours could provide new insights in the investigation of such critical elements.

Author Contributions: M.V.T. collected the samples; A.V.K. found the new mineral; F.N. performed the X-ray structural investigations; R.Š. and A.V.K. conducted the electron-microprobe analyses; A.A.A. and V.Y.K. determined the optical, physical, and chemical properties; and A.V.K., F.N. and J.P. wrote the paper.

Acknowledgments: The reviewers and Guest Editor Cristian Biagioni are acknowledged for their constructive comments.

Conflicts of Interest: The authors declare no conflict of interest.

References

- Pašava, J.; Pertlik, F.; Stumpfl, E.F.; Zemann, J. Bernardite, a new thallium arsenic sulphosalt from Allchar, Macedonia, with a determination of the crystal structure. *Mineral. Mag.* **1989**, *53*, 531–538. [[CrossRef](#)]
- Johan, Z.; Mantienne, J.; Picot, P. La chabournéite, un nouveau minéral thallifère. *Bull. Minér.* **1981**, *104*, 10–15.
- Radtke, A.S.; Dickson, F.W.; Slack, J.F.; Brown, K.L. Christite, a new thallium mineral from the Carlin gold deposit, Nevada. *Am. Mineral.* **1977**, *62*, 421–425.
- Nestola, F.; Guastoni, A.; Bindi, L.; Secco, L. Dalnegroite, $\text{Tl}_{5-x}\text{Pb}_{2x}(\text{As,Sb})_{21-x}\text{S}_{34}$, a new thallium sulphosalt from Lengenbach quarry, Binntal, Switzerland. *Mineral. Mag.* **2009**, *73*, 1027–1032. [[CrossRef](#)]
- Johan, Z.; Picot, P.; Hak, J.; Kvaček, M. La parapiérotite, un nouveau minéral thallifère d'Allchar (Yougoslavie). *Tsch. Mineral. Petrogr. Mitt.* **1975**, *22*, 200–210. [[CrossRef](#)]
- Johan, Z.; Pierrot, R.; Schubnel, H.J.; Permingeat, F. La picotpaulite TlFe_2S_3 , une nouvelle espèce minérale. *Bull. Soc. Fr. Minéral. Crist.* **1970**, *93*, 545–549.
- Graeser, S.; Berlepsch, P.; Makovicky, E.; Balić-Zunić, T. Sicherite, $\text{TlAg}_2(\text{As,Sb})_3\text{S}_6$, a new sulfosalt mineral from Lengenbach (Binntal, Switzerland): Description and structure determination. *Am. Mineral.* **2001**, *86*, 1087–1093. [[CrossRef](#)]
- Sazonov, V.N.; Murzin, V.V.; Grigor'ev, N.A. Vorontsovsk gold deposit: An example of carlin-type mineralization in the Urals, Russia. *Geol. Ore Depos.* **1998**, *40*, 139–151.
- Plášil, J.; Kasatkin, A.V.; Škoda, R.; Stepanov, S.Y. Parapiérotite from the Vorontsovskoe gold deposit, Northern Urals, Russia: Crystal structure and chemical composition. *Zapiski RMO* **2018**, *1*, 68–78.
- Murzin, V.V.; Bushmakin, A.F.; Sustavov, S.G.; Shcherbachov, D.K. Clerite MnSb_2S_4 —A new mineral from Vorontsovskoye gold deposit in the Urals. *Zapiski VMO* **1996**, *125*, 95–101.
- Angel, R.J.; Nestola, F. A century of mineral structures: How well do we know them? *Am. Mineral.* **2016**, *101*, 1036–1045. [[CrossRef](#)]
- Holland, T.J.B.; Redfern, S.A.T. Unit cell refinement from powder diffraction data: The use of regression diagnostics. *Mineral. Mag.* **1997**, *61*, 65–77. [[CrossRef](#)]
- Nolze, G.; Kraus, W. PowderCell 2.0 for Windows. *J. Powder Diffr.* **1998**, *13*, 256–259.
- Sheldrick, G.M. A short history of SHELX. *Acta Crystallogr. Sect. A* **2008**, *64*, 112–122. [[CrossRef](#)] [[PubMed](#)]
- Biagioni, C.; Bindi, L.; Zaccarini, F. Crystal chemistry of mercury sulfosalts-galkhaite, $(\text{Hg}_{5+x}\text{Cu}_{1-x})\text{Cs}_{1-x}\text{As}_4\text{S}_{12}$ ($x \approx 0$): Crystal structure and revision of the chemical formula. *Can. Mineral.* **2014**, *52*, 873–882. [[CrossRef](#)]

16. Makovicky, E. Micro- and mesoporous sulfide and selenide structures. *Rev. Mineral. Geochem.* **2005**, *57*, 403–434. [[CrossRef](#)]
17. Divijakovic, V.; Nowacki, W. Die Kristallstruktur von Galchait $[\text{Hg}_{0.76}(\text{Cu,Zn})_{0.24}]_{12}\text{Tl}_{0.96}(\text{AsS}_3)_8$. *Z. Kristallogr.* **1975**, *142*, 262–270.
18. Chen, T.T.; Szymański, J.T. The structure and chemistry of galkhaite, a mercury sulfosalt containing Cs and Tl. *Can. Mineral.* **1981**, *19*, 571–581.
19. Shannon, R.D. Revised effective ionic radii and systematic studies of interatomic distances in halides and chalcogenides. *Acta Crystallogr. Sect. A* **1976**, *32*, 751–767. [[CrossRef](#)]
20. Grudzev, V.S.; Stepanov, V.I.; Shumkova, N.G.; Chernitsova, M.M.; Yudin, R.N.; Bryzgalov, I.A. Galkhaite, HgAsS_2 , a new mineral from arsenic-antimony-mercury deposits of the USSR. *Doklady Akademii Nauk SSSR* **1972**, *205*, 1194–1197. (In Russian)
21. Mills, S.J.; Hatert, F.; Nickel, E.H.; Ferraris, G. The standardisation of mineral group hierarchies: Application to recent nomenclature proposals. *Eur. J. Mineral.* **2009**, *21*, 1073–1080. [[CrossRef](#)]
22. Vasilyev, V.I.; Pervukhina, N.V.; Borisov, S.V.; Magarill, S.A. New data on composition and crystal structure of galkhaite $(\text{Hg,Cu})_6(\text{Cs,Tl})(\text{As,Sb})_4\text{S}_{12}$. *Zapiski RMO* **2009**, *138*, 83–92. (In Russian) [[CrossRef](#)]
23. Pekov, I.V.; Bryzgalov, I.A. New data on galkhaite. *New Data Miner.* **2006**, *41*, 26–32.
24. Ober, J.A. *Mineral commodity summaries 2018*; U.S. Geological Survey: Reston, VA, USA, 2018; pp. 168–169.
25. Biagioni, C.; Bonaccorsi, E.; Moëlo, Y.; Orlandi, P.; Bindi, L.; D’Orazio, M.; Vezzoni, S. Mercury-arsenic sulfosalts from the Apuan Alps (Tuscany, Italy). II. Arsiccioite, $\text{AgHg}_2\text{TlAs}_2\text{S}_6$, a new mineral from the Monte Arsiccio mine: Occurrence, crystal structure and crystal chemistry of the routhierite isotypic series. *Mineral. Mag.* **2014**, *78*, 101–117. [[CrossRef](#)]
26. Johan, Z.; Mantienne, J.; Picot, R. La routhiérite, TlHgAsS_3 , et la laffittite, AgHgAsS_3 , deux nouvelles espèces minérales. *Bull. Soc. Fr. Minéral.* **1974**, *97*, 48–53.
27. Engel, P.; Nowacki, W.; Balić-Žunić, T.; Šćavnićar, S. The crystal structure of simonite, $\text{TlHgAs}_3\text{S}_6$. *Z. Kristallogr.* **1982**, *161*, 159–166. [[CrossRef](#)]
28. Graeser, S.; Schwander, H.; Wulf, R. Stalderite $\text{TlCu}(\text{Zn,Fe,Hg})_2\text{As}_2\text{S}_6$ —A new mineral related to routhierite: Description and crystal structure determination. *Schweiz. Mineral. Petrogr. Mitt.* **1995**, *75*, 337–345.
29. Ježek, B. Vrbait, ein neues Thalliummineral von Allchar in Macedonien. *Z. Kristallogr.* **1912**, *51*, 365–378. [[CrossRef](#)]

